Experimental observation of the characteristic relations of type-I intermittency in the presence of noise

Jin-Hang Cho,[1,2] Myung-Suk Ko,[1] Young-Jai Park,[2,*] and Chil-Min Kim[1,†]
[1]*National Creative Research Initiative Center for Controlling Optical Chaos, Department of Physics, Paichai University, Taejon 302-735, Korea*
[2]*Department of Physics, Sogang University, Seoul 121-742, Korea*
(Received 6 July 2001; published 1 March 2002)

Recently, it has been reported that the characteristic relation of type-I intermittency in the presence of noise is deformed nontrivially as the channel width ϵ changes from the positive region to the negative. In order to verify it experimentally as a real phenomenon, we study the characteristic relations both for $\epsilon<0$ and for $\epsilon>0$ in a simple inductor-resistor-diode circuit that is under noisy circumstances. The experimental results agree well with the theoretical expectation that the characteristic relations are $\langle l\rangle \propto \epsilon^{-1/4}$ for $\epsilon>0$ and $\langle l\rangle \propto \exp(\alpha|\epsilon|^{3/2})$ for $\epsilon<0$.

DOI: 10.1103/PhysRevE.65.036222 PACS number(s): 05.45.Pq, 07.50.−e

I. INTRODUCTION

In nonlinear dynamical systems, it is readily observed that long quasiregular signals are interrupted by short chaotic bursts irregularly. The phenomenon, so-called intermittency, has been extensively studied for a long time because it is an important route to chaos along with period doubling, quasiperiodicity, and crisis. Pomeau and Manneville classified it into three types, types I, II, and III, in terms of the structure of the local Poincaré map, $x_{n+1}=x_n+ax_n^2+\epsilon$, $x_{n+1}=(1+\epsilon)x_n+ax_n^3$, and $x_{n+1}=-(1+\epsilon)x_n-ax_n^3$, respectively [1–4]. And they obtained the characteristic relations of them, which are $\langle l\rangle \propto \epsilon^{-1/2}$ for type I and $\langle l\rangle \propto \epsilon^{-1}$ for types II and III, where $\langle l\rangle$ is the average laminar length, the parameter ϵ in type-I intermittency is the channel width between the diagonal and the local Poincaré map, and $1+\epsilon$ in types II and III is the slope of the local Poincaré map around the tangent point [1–3,5]. In a more recent study it was known that characteristic relations of intermittency depend not only on the structure of the local Poincaré map but on the reinjection probability distribution (RPD). Accordingly, the characteristic relation of type-I intermittency is of the form $\langle l\rangle \propto \epsilon^{-\nu}(0<\nu\leqslant\frac{1}{2})$ or $\langle l\rangle \sim -\ln\epsilon$ [6,7], and that of types II and III is of the form $\langle l\rangle \propto \epsilon^{-\nu}$ $(\frac{1}{2}\leqslant\nu\leqslant 1)$ depending on the RPD [8].

Along with that, other authors have studied characteristic relations of intermittency in the presence of noise, which is unavoidable in real systems. Eckmann *et al.* studied them in the region $\epsilon>0$ and extended their result to the region $\epsilon<0$ [10]. So they were misled to the idea that the characteristic relation is trivially related to the change of signs of the channel width. Hirsch *et al.* also studied the subject by using a Fokker-Planck equation [11] and adopting renormalization group analysis [12], but obtained the characteristic relations only in the region $\epsilon>0$. Very recently, Kye and Kim have theoretically obtained the characteristic relations of type-I intermittency in the presence of noise in the region $\epsilon<0$ by using a Fokker-Planck equation. They have found the characteristic relation changes nontrivially as the parameter ϵ moves from the positive region to the negative [13].

This characteristic relation is very important in analyzing experimental results of a system where noise accompanies intrinsically. For example, a gain-modulated CO_2 laser produces type-I intermittency when the operating frequency is deviated from the gain line center [14]. This result cannot be explained satisfactorily without the above characteristic relation because the system is affected by intrinsic noise such as quantum noise, pumping noise, etc. [15]. So it is necessary to verify the characteristic relation experimentally, which has never been tried yet.

In this paper, we purpose to observe experimentally the deformation of the characteristic relation of type-I intermittency in the presence of noise that Kye and Kim studied theoretically. For the experiment, we use a simple inductor-resistor-diode (IRD) circuit where all the parameters including noise amplitude can be precisely controlled with ease. Section II describes an analytic solution following Refs. [6,13], and Secs. III and V show numerically and experimentally the characteristic relation of type-I intermittency in the presence of noise.

II. THEORETICAL BACKGROUND

When the local Poincaré map of type-I intermittency in the presence of noise is given [2,3,6,8,9,11,12,16],

$$x_{n+1}=x_n+ax_n^2+\epsilon+\sqrt{2D}\xi_n \quad (a>0), \tag{1}$$

the characterisitic relation can be obtained for two cases of the channel width $\epsilon>0$ and $\epsilon<0$. Here D is the dispersion of Gaussian white noise ξ_n.

For $\epsilon\gg D>0$, noise can be neglected since the channel widths mainly contribute to the characteristic relation. So the characteristic relation can be obtained by solving the general form of type-I intermittency $x_{n+1}=x_n+ax_n^2+\epsilon$. On the other hand for $\epsilon<0$, Eq. (1) can be transformed into a differential form $\dot{x}=-dV(x)/dx+\sqrt{2D}\xi(t)$, where $dV(x)/dx=-ax^2-\epsilon$ and $\dot{x}=x_{n+1}-x_n$ in the long laminar length approximation.

*Electronic address: yjpark@ccs.sogang.ac.kr
†Electronic address: chmkim@mail.paichai.ac.kr

When we neglect the effect of noise for $\epsilon \gg 0$, the characteristic relation of type-I intermittency can be obtained by integrating $dx/dt = ax^2 + \epsilon$ under the long laminar length approximation. If we give a gate that sets an acceptance $|y_{in}| \leqslant c$ on deviations in the laminar region, the laminar length $l(y_{in}, c)$ for the reinjection at y_{in} becomes

$$l(y_{in}, c) = \frac{1}{\sqrt{a\epsilon}} \left[\tan^{-1}\left(\sqrt{\frac{a}{\epsilon}} c \right) - \tan^{-1}\left(\sqrt{\frac{a}{\epsilon}} y_{in} \right) \right].$$

Then the average laminar length is given by

$$\langle l \rangle = l(0,c) \int_{-\Delta}^{0} P(y_{in}) dy_{in} + \int_{0}^{c} l(y_{in}, c) P(y_{in}) dy_{in},$$

where $-\Delta$ is the value of y_{in} representing the lower bound of the reinjection (LBR).

From the above equation we can obtain various characteristic relations according to the RPD that is given by $P(y_{in})$. When the LBR is below the tangent point, the above equation can be written as

$$\langle l \rangle = \frac{1}{\sqrt{a\epsilon}} \tan^{-1}\left(\sqrt{\frac{a}{\epsilon}} c \right) \propto \epsilon^{-1/2},$$

which is irrespective of the RPDs, because the first term is dominant. On the contrary when the LBR is above the tangent point, the first term vanishes and the second term converges to a constant as $\epsilon \to 0$. And if the LBR is at the tangent point, various characteristic relations can be obtained. When RPD is fixed, the characteristic relation has the same form as the case below. In the case of the nonuniform RPD of the form $1/(2\sqrt{\delta + c}\sqrt{y_{in} + \delta})$, the characteristic relation is given by

$$\langle l \rangle = \frac{i\sqrt{-i\sqrt{\epsilon}}}{a^{3/4}\sqrt{c\sqrt{\epsilon}}} \left[\tan^{-1}\left(\frac{a^{1/4}\sqrt{c}}{\sqrt{i\sqrt{\epsilon}}} \right) - \tan^{-1}\left(\frac{a^{1/4}\sqrt{c}}{\sqrt{-i\sqrt{\epsilon}}} \right) \right] + \text{c.c.},$$

where c.c. denotes the complex conjugate. This characteristic relation has a real value and is the form $\langle l \rangle \propto \epsilon^{-1/4}$ as $\epsilon \to 0$. And when the RPD is uniform, in the same manner, we can obtain a characteristic relation such that $\langle l \rangle \propto \ln(\epsilon)$ as $\epsilon \to 0$. Thus we understand that the characteristic relation depends only on the RPD when $\epsilon \gg 0$ although noise is applied.

On the other hand, when $\epsilon < 0$, we can approximate the difference Eq. (1) in the long laminar region to the stochastic differential equation as follows [11]:

$$\dot{x} = -V'(x) + \sqrt{2D}\xi(t), \tag{2}$$

where the dot and prime denote differentiation with respect to t and x, respectively, $\xi(t)$ is the Gaussian white noise such that $\langle \xi(t')\xi(t) \rangle = \delta(t' - t)$ and $\langle \xi(t) \rangle = 0$ [17], and $V(x)$ is the potential given by $V(x) = -\frac{1}{3}ax^3 - \epsilon x + c$, where c is the integration constant. The above equation can be considered as the equation of motion of the point particle under the potential $V(x)$ and random perturbation $\xi(t)$.

From the above stochastic differential equation, we obtain the backward Fokker-Planck equation (FPE) [11,17] in the well-established procedure [17] as follows:

$$\frac{\partial G(x,t)}{\partial t} = -V'(x)\frac{\partial G(x,t)}{\partial x} + D\frac{\partial^2 G(x,t)}{\partial x^2}, \tag{3}$$

where $G(x,t)$ is the probability density of the particle at $\{x,t\}$. After integrating the above FPE, we obtain a mean first-passage time (MFPT) as follows [11,17]:

$$-1 = -V'(x)\frac{dT}{dx} + D\frac{d^2T}{dx^2}, \tag{4}$$

where $T(x)$ is the mean escaping time defined by $T(x) = \langle t \rangle = -\int_0^\infty t(\partial G(x,t)/\partial t)dt$ under the boundary conditions that $G(x,0) = 1$ and $\lim_{t\to\infty} G(x,t) = 0$. The MFPT function $T(x)$ is the average transition time from the reinjection to the escaping point of the particle under the potential $V(x)$ and random perturbation.

The general solution of Eq. (3) can be derived as follows:

$$T(x) = c\int_{x_l}^{x} dx' \exp\left\{ \frac{1}{D}V(x') \right\} - \frac{1}{D}\int_{x_l}^{x} dx' \int_{x_l}^{x'} dx'' \exp\left\{ \frac{1}{D}[V(x') - V(x'')] \right\}, \tag{5}$$

where c is the integration constant, x_l is the lower bound of the laminar phase, and x is the destination point of the transition. We can easily verify that Eq. (5) is the general solution for the MFPT equation by inserting Eq. (5) into Eq. (4).

If noise is small enough such that $D \ll 1$, the first term in the above equation is suppressed by the factor of $1/D$ and the second term becomes dominant. The second term is not integrable analytically. Then we can expand approximately the potential at the extremal points $x_\pm$ such that $V(x) \approx V(x_\pm) + (V''(x_\pm)/2)(x - x_\pm)^2 + O([x - x_\pm]^3)$.

In that case, the MFPT function $T(x)$ can be approximated as follows:

$$T(x) \approx -\frac{1}{D}\exp\left\{ \frac{1}{D}[V(x_+) - V(x_-)] \right\} \times \int_{x_l}^{x} dx' \int_{x_l}^{x'} dx'' \exp\left\{ \frac{1}{2D}[V''(x_+)(x' - x_+)^2 - V''(x_-)(x'' - x_-)^2] \right\}. \tag{6}$$

The extremal points are given by $x_\pm = \pm\sqrt{-\epsilon/a}$ in Eq. (2). In the far outside of the laminar phase (i.e., at the limit $x \to \infty$ and $x_l \ll x_-$), we can perform the integration of the quadratic exponent [17] and then obtain the following approximated solution of the MFPT equation:

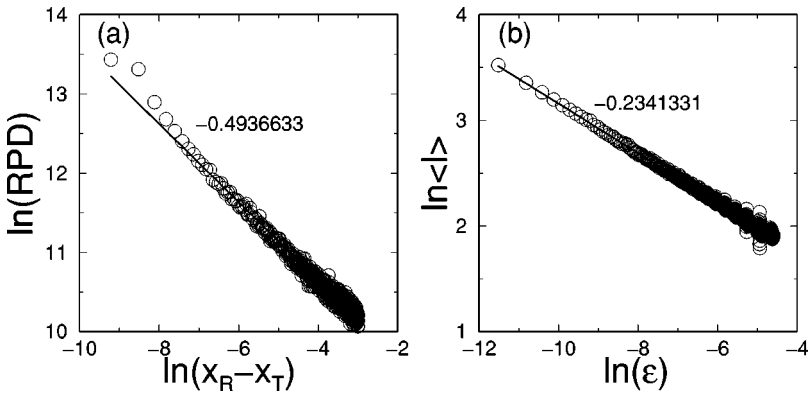

FIG. 1. The RPD and the characteristic relation in the absence of noise. (a) The RPD shows a slope of $-\frac{1}{2}$ and (b) the characteristic relation is well fitted to the slope $-\frac{1}{4}$ that is the exponent when the RPD is of the form $1/\sqrt{x}$.

$$|T| = \frac{\pi}{\sqrt{a|\epsilon|}} \exp\left\{ \frac{4}{3D\sqrt{a}} |\epsilon|^{3/2} \right\} \quad \text{for} \quad \epsilon < 0. \tag{7}$$

Thus the characterisitc relation becomes

$$\langle l \rangle \propto \langle l \rangle_0 \exp\left\{ \frac{4}{3D\sqrt{a}} |\epsilon|^{3/2} \right\}. \tag{8}$$

III. NUMERICAL SIMULATION

Now we study the deformation of the characteristic relations from $\langle l \rangle \propto \epsilon^{-1/4}$ to $\langle l \rangle \propto \langle l \rangle_0 \exp[(4/3D\sqrt{a})|\epsilon|^{3/2}]$ when the RPD is of the form $1/\sqrt{y_{in}}$ by using an illustrating model of a logistic map

$$x_{n+1} = F(A,B;x_n) = f^A[f^B(x_n)],$$

where $f^A(x_n) = 4Ax_n(1-x_n)$ and $f^B(x_n) = 4Bx_n(1-x_n)$. In the map, the critical value of parameter B_c at which tangent bifurcation occurs is

$$\frac{-9\sqrt{A} + 8A^{3/2} + (4A-3)^{3/2}}{16\sqrt{A}(A-1)},$$

and the tangent point x_c is

$$\frac{2}{3} - \frac{\sqrt{4-3/B_c}}{6}.$$

Since the chaotic band near B_c is bounded in the range $[x_L, x_U]$, the point of LBR is the tangent point $x_c = x_L = 0.563\,066\,00\ldots$ at $A = A_t = 0.941\,461\,94\ldots$. Here $x_U = F(A,B_c;x_M) = A$, where x_M is a point satisfying $dF(A,B_c;x_M) = 0$ and $x_L = F(A,B_c;x_U)$. We are interested in the characteristic relation, the change of the average laminar length according to the departure of B from B_c, i.e., $\epsilon = B_c - B$ for a fixed value of A.

Figures 1(a) and 1(b) show the RPD and the characterisitc relations, respectively, in the absence of noise. The slope of the RPD in the logarithmic scale is obtained by dividing the gate into 1000 sections and by counting the number of reinjections at each section. As is shown in the figure, the slope

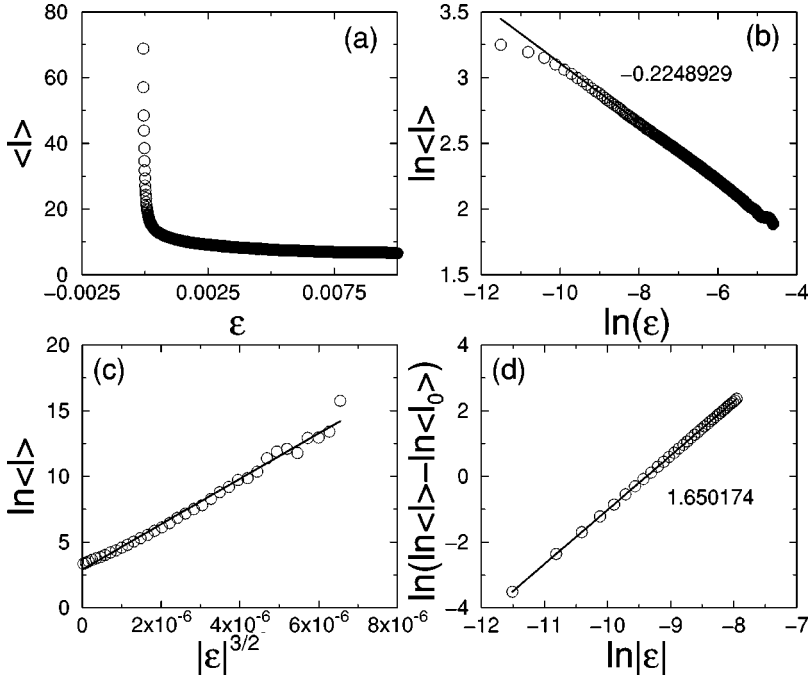

FIG. 2. The characteristic relations of the average laminar length versus $|\epsilon|$ in the presence of noise. (a) is for whole range, (b) for $\epsilon > 0$, and (c) and (d) for $\epsilon < 0$.

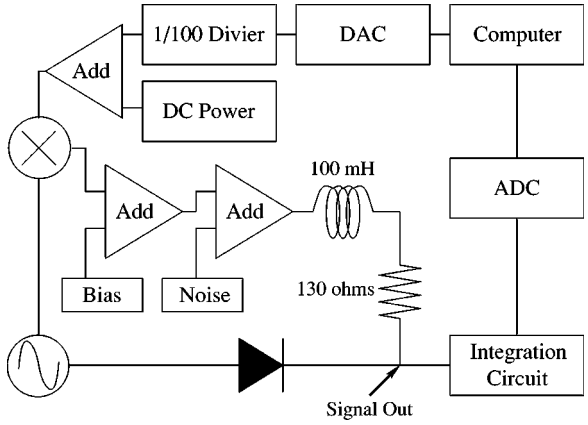

FIG. 3. Schematic diagram of experimental setup.

is well fitted to the $-1/2$ slope. The slope of the average laminar length according to the channel width is also well fitted to the $-1/4$ slope. From these, we can understand that the RPD is of the form $1/\sqrt{x}$, and the LBR is at the tangent point.

The scaling relation of the laminar length in the presence of noise is studied by applying small 5.0×10^{-3} noise to the above map such that $x_{n+1}=f^A[f^B(x_n)]+D\xi_n$. In this map since RPD is of the form $1/\sqrt{x}$, the characterisitic relations of the average laminar length will be deformed from $\langle l\rangle \propto \epsilon^{-1/4}$ for $\epsilon \gg 0$ to $\langle l\rangle \propto \langle l\rangle_0 \exp[(4/3D\sqrt{a})|\epsilon|^{3/2}]$ for $\epsilon<0$. Figure 2 shows the characterisitic relations of the average laminar length according to the channel width ϵ. As is shown in Fig. 2(b), the slope is well fitted to $-1/4$ slope when $\epsilon \gg 0$. On the contrary, as shown in Fig. 2(d), when $\epsilon<0$, the slope is well fitted to the 3/2 slope that is the exponent of the exponential term of Eq. (7). So in this map the characterisitic relation deforms from $\langle l\rangle \propto \epsilon^{-1/4}$ to $\langle l\rangle \propto \langle l\rangle_0 \exp[(4/3D\sqrt{a})|\epsilon|^{3/2}]$ as ϵ changes from positive to negative. Another evidence of deformation from $\langle l\rangle \propto \epsilon^{-1/2}$ to $\langle l\rangle \propto \langle l\rangle_0 \exp[(4/3D\sqrt{a})|\epsilon|^{3/2}]$, when RPD is fixed at the tangent point, was already studied by Kye and Kim [13]. From these results we can understand that the characteristic relation of type-I intermittency in the presence of noise deforms from $\langle l\rangle \propto \epsilon^{-\nu}$ $(0<\nu\leqslant\frac{1}{2})$ or $\langle l\rangle \sim -\ln\epsilon$ for $\epsilon \gg 0$ to $\langle l\rangle \propto \langle l\rangle_0 \exp[(4/3D\sqrt{a})|\epsilon|^{3/2}]$ for $\epsilon<0$.

IV. EXPERIMENT SETUP

In the experiment, we use a simple IRD circuit where all the parameters including noise amplitude can be precisely controlled with ease.

A simple electronic circuit consisting of an inductor (100 mH), a resistor (130 Ω), and a silicon junction diode (1N4007) is connected in series as given in Fig. 3. A dc voltage in the range between ±10V from a digital-analog (DA) converter [National Instruments PCI-MIO-16E-1 with an analog-digital (AD) converter] is reduced to 1/100 with a voltage divider to control the amplitude of the driving signal precisely. The DA converter with 12-bit resolution is controlled by a pentium-II personal computer. The reduced voltage is added to another dc voltage and the total dc voltage is multiplied by a sinusoidal signal from a function generator (Tektronix, FG 501A) by using a multiplier (MPY100), of amplitude 1.0 V. We add a 0.7 V bias voltage and a random noise signal from a random signal generator (HP 33120A). The total signal is applied to the simple electronic circuit. The frequency from the function generator and the bias volt-

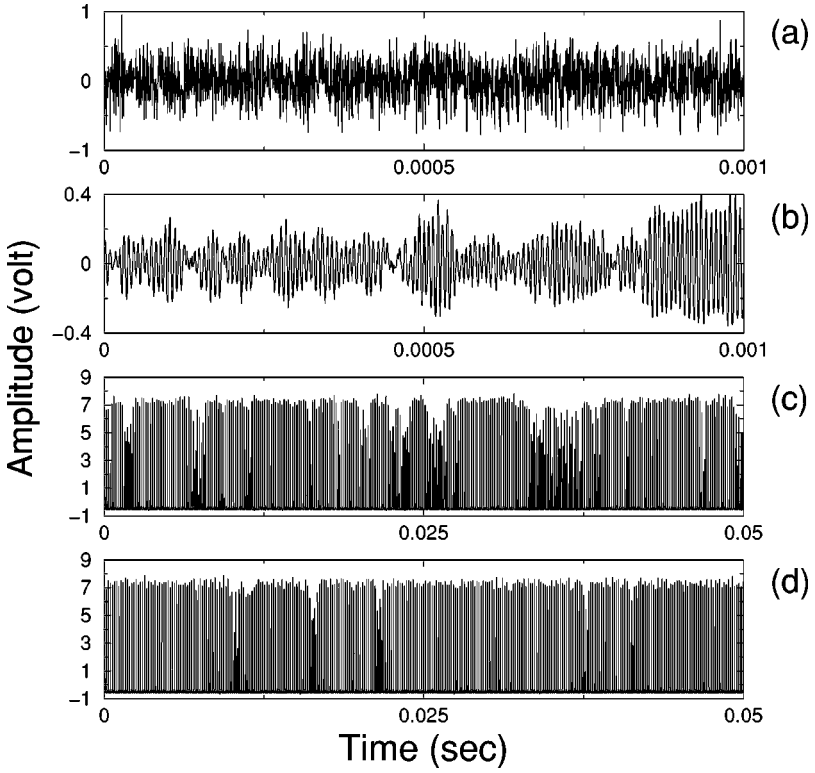

FIG. 4. Temporal behavior of noise and type-I intermittency. (a) 1.0-V noise from the function generator, (b) noise across the diode, (c) and (d) type-I intermittency in the presence of 1.0-V noise when the amplitude of the driving signal is 3.50 V and 3.55 V, respectively.

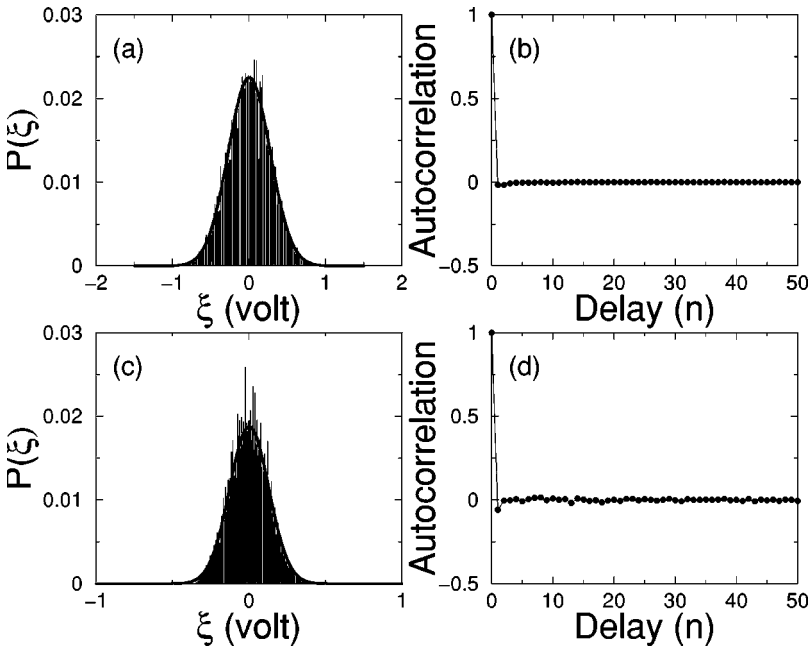

FIG. 5. Distributions and autocorrelations of noise. (a) and (b) are for the noise from the noise generator and (c) and (d) for the noise across the diode.

age are fixed at 18 kHz and 0.7 V, respectively. All the external signals are added with operational amplifiers (LM353). Through this configuration we can change the amplitude of the driving signal by 0.03 mV at each step.

To obtain the desired experimental data, each rectified pulse is integrated with an integrating circuit. We add a 0.6 V dc voltage to the rectified pulses before integration because the voltage drop of the silicon diode is -0.6 V when it is conducting. The rectified voltages are reduced with a variable resistor in order to prevent distortion due to the peak of the integrated voltage being higher than 15 V. Here since the peaks of the rectified pulses correspond to those of the integrated pulses, the peaks of the integrated pulses are stored in the computer through an AD converter. The digitizing frequency of the AD converter is 150 kHz. The chaotic outputs of the rectified and the integrated pulses are also monitored by using a digital storage oscilloscope (LeCroy 9310).

V. EXPERIMENTAL RESULTS AND DISCUSSIONS

The circuit exhibits various chaotic behaviors due to the nonlinear capacitance of the junction diode [18]. From the circuit we obtain the typical temporal behaviors of the noise from the function generator, the noise across the diode, and type-I intermittency in the presence of noise near the period-3 window as given in Fig. 4. When noise of amplitude 1.0 V [Fig. 4(a)] is applied to the circuit after the driving signal is turned off, the amplitude of the noise across the diode is reduced to 0.4 V as given in Fig. 4(b) due to the inductor and the capacitance of the diode. This reduced noise is the real one affecting the characteristic relation of type-I intermittency in this circuit. When the driving signal is turned on, we can observe that almost regular rectified pulses across the diode are interrupted irregularly by chaotic bursts as shown in Figs. 4(c) and 4(d). When the amplitude of the driving signal is 3.50 V, the circuit exhibits a short period of regular rectified pulses. But when the amplitude is increased up to 3.55 V, the circuit exhibits a long period of regular rectified pulses. The maximum amplitude, about 7.8 V, of the rectified signals is much higher than the amplitude of the noise across the diode. From the figures, we can understand that the noise that affects the rectified pulses is about 5% in our experiment.

Next we obtain the probability distributions and autocorrelations of the noise from the noise generator and the noise across the diode. As shown in Figs. 5(a) and 5(b) the noise

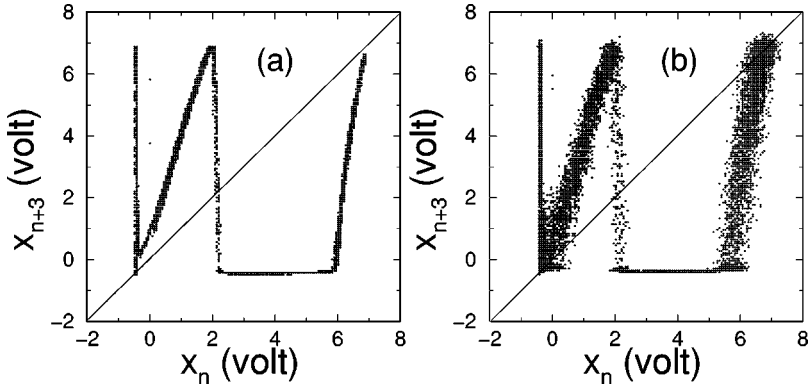

FIG. 6. x_n versus x_{n+2} return maps when (a) noise is absent and (b) 1.0-V noise is applied. The amplitude of the driving signal is 3.5-V.

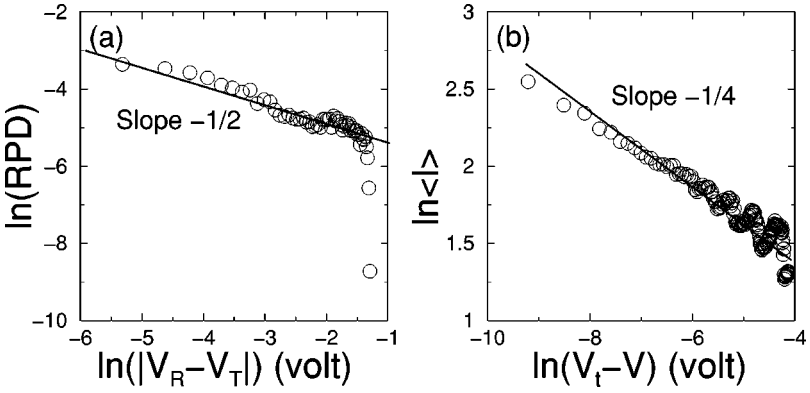

FIG. 7. The RPD and the characteristic relation in the absence of noise. (a) the RPD shows a slope of $-\frac{1}{2}$ when the amplitude of driving signal is 3.507 V and (b) the characteristic relation shows the $-\frac{1}{4}$ slope that is the exponent for the RPD of the form $1/\sqrt{x}$.

from the noise generator is well fitted to the Gaussian profile and is δ correlated. This means that the external noise can be regarded as Gaussian white noise. The noise across the diode that is taken at every average period of 5 μsec is also well fitted to the Gaussian profile and is δ correlated as shown in Figs. 5(c) and 5(d). Thus the noise affecting the circuit can be regarded as Gaussian white noise.

From the temporal behavior of type-I intermittency, we obtain the x_n versus x_{n+2} return map as shown in Fig. 6 whenthe amplitude of the driving signal is 3.5 V. The return map on the right-hand side in Fig. 6(a) does not touch the diagonal line when the noise generator is turned off. However when the noise generator is turned on, a broad curve on the right-hand side crosses the diagonal line, as shown in Fig. 6(b), due to the noise. This is the typical feature of the return map of type-I intermittency in the presence of noise having a quadratic structure [7]. Here the tangent point is at about 7.2 V.

In order to show the characteristic relation in the absence of noise, we obtain the reinjection probability distribution and the characteristic relation for $\epsilon>0$. When the amplitude of the driving signal is 3.507 V, after the noise generator is turned off, we obtain the RPD by dividing the reinjection region from 7.2 V to 6.7 V into 100 sections. Figure 7(a) is the log-log plot of the total number of reinjections at each section versus $|V_R-V_T|$, where V_R is the amplitude of reinjection and V_T is the amplitude of the tangent point. As given in the figure, the slope of the RPD is about $-1/2$ when $|V_R-V_T|$ is small, which means that the RPD related to our experiment is of the form $1/\sqrt{x}$.

To observe the characteristic relation, the average laminar length is obtained according to the amplitude of the driving signal for $\epsilon>0$ without noise. In this experiment, we increase the dc voltage from the DA converter by 0.03 mV at each step for fine tuning. As the amplitude of the driving signal increases, the length of the laminar phase is counted and the data are stored in the computer. From the data we can find the bifurcation point V_t by searching for the last point where the chaotic burst appears. The bifurcation point, determined from the experimental data, is $V_t=3.54$ V. Average laminar length at V_t is about 10^3 in our circuit. The log-log plot of average laminar length versus ϵ, where $\epsilon=V_t-V>0$, is given in Fig. 6(b). In the figure the circles are experi-

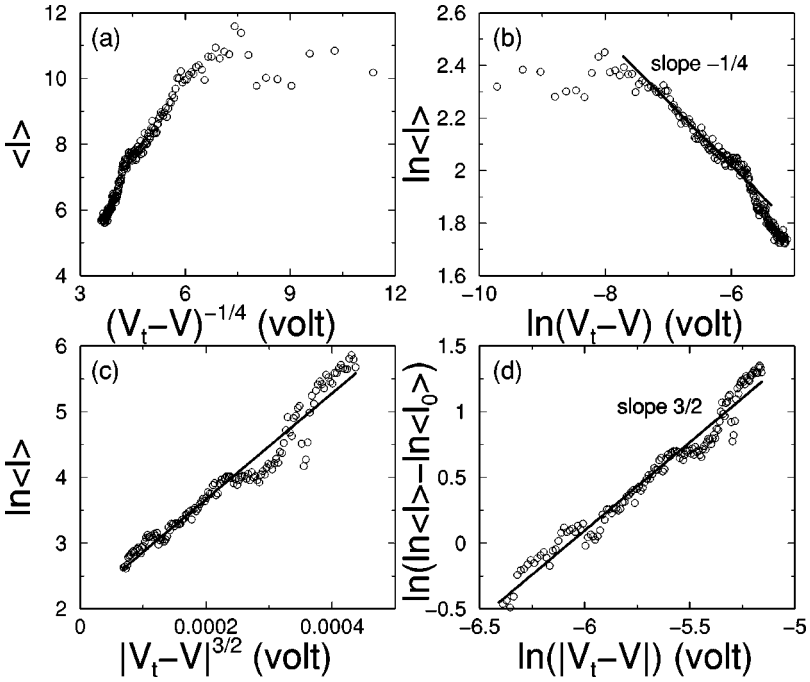

FIG. 8. The characteristic relation of the average laminar length versus $|V_t-V|$ in the presence of 1.0-V noise. (a) and (b) for $\epsilon>0$ and (c) and (d) for $\epsilon<0$.

mental results and the dashed line is the slope of $-1/4$. So the measured average laminar length is well fitted to the theoretically expected slope. In this experiment, without noise one cannot observe the typical behavior of intermittency for the region of $V<V_t$.

Now, the noise generator is turned on and the average laminar length is measured according to the amplitude of the driving signal when the noise amplitude is 1.0 V. The data are stored in the computer. In the experiment, we are able to measure a laminar phase length of 1.2×10^5 at most because of the limit of computer memory. So the range of the driving signal amplitude for which we have studied the characteristic relations is from 3.5070 V to 3.6072 V.

As shown in Fig. 8, we obtain the characteristic relations for two regions $\epsilon>0$ and $\epsilon<0$. The experimental data of the average laminar length versus $V-V_t$ for $\epsilon>0$ are given in Figs. 8(a) and 8(b). In Fig. 8(a) the plot of $\langle l\rangle$ versus $(V_t-V)^{-1/4}$ shows a linear curve for $V\ll V_t$. To see it more clearly we obtain the slope in the logarithmic scale. Figure 8(b) shows that the slope of the experimental data is well fitted to the $-1/4$ slope of the solid line. This means that the characteristic relation is $\langle l\rangle\propto\epsilon^{-1/4}$ for $V\ll V_t$. This is the very characteristic relation for $\epsilon\gg D>0$ that was obtained in the previous theoretical analysis [4]. The figure also shows that $\langle l\rangle$ approaches $\langle l_0\rangle$ as V approaches V_t because of the deformation.

Figures 8(c) and 8(d) show the characteristic relation for the region $V>V_t$. As shown in Fig. 8(c), the plot of $\ln\langle l\rangle$ versus $|V_t-V|^{3/2}$ shows a linear curve. To show the characteristic relation more clearly, we obtain the y interception of $\ln\langle l_0\rangle$ from Fig. 8(c) by linear regression of the curve. $\ln\langle l_0\rangle$ is about 2.0. The plot of $\ln(\ln\langle l\rangle-\ln\langle l_0\rangle)$ versus $\ln|V_t-V|$ is well fitted to the slope of 3/2 as given in Fig. 8(d). It means that the characteristic relation obtained in the experiment agrees well with the theoretical one [13], i.e., $\langle l\rangle\propto\langle l\rangle_0\exp(\alpha|V-V_t|^{3/2})$. From the above figures we explicitly understand that the characteristic relations are $\langle l\rangle\propto\epsilon^{-1/4}$ for $V\ll V_t$, $\langle l\rangle\sim\langle l_0\rangle$ for $V\lesssim V_t$, and $\langle l\rangle\propto\langle l\rangle_0\exp(\alpha|V-V_t|^{3/2})$ for $V>V_t$.

It seems appropriate to comment on why our experimental result is different from the theoretical prediction of Ref. [13] for the case of the $\epsilon>0$ regime. In fact, while our experimental result belongs to the case having the RPD of the form $1/x^{1/2}$, the theoretical one has used the fixed RPD.

VI. CONCLUSION

In conclusion, we have experimentally observed the characteristic relations of type-I intermittency in the presence of noise according to the channel width in a simple IRD circuit. First, we have shown that, in the absence of noise, the characteristic relation is $\langle l\rangle\propto\epsilon^{-1/4}$ due to the RPD of the form $x^{-1/2}$. Then, we have observed the characteristic relations in the presence of noise, that is, $\langle l\rangle\propto\epsilon^{-1/4}$ for $\epsilon\gg0$, $\langle l\rangle\sim\langle l_0\rangle$ for $\epsilon\gtrsim0$, and $\langle l\rangle\propto\exp|\epsilon|^{3/2}$ for $\epsilon<0$. These results show that the theoretically predicted characteristic relations of type-I intermittency in the presence of noise [13] are actually observable in a real chaotic dynamical system under noisy circumstances.

Finally, through further investigation it is interesting to find the experimental phenomenon having the fixed RPD, which corresponds to another theoretical prediction $\langle l\rangle\propto\epsilon^{-1/2}$ for the case of the $\epsilon>0$ regime in Ref. [13].

ACKNOWLEDGMENT

This work was supported by the Creative Research Initiatives of the Korean Ministry of Science and Technology.

[1] Y. Pomeau and P. Manneville, Commun. Math. Phys. **74**, 189 (1980); H. Kaplan, Phys. Rev. Lett. **68**, 553 (1992); J.E. Hirsch, B.A. Hubetman, and J. Scalapino, Phys. Rev. A **25**, 519 (1982); P. Berg, M. Dubois, P. Manneville, and Y. Pomeau, J. Phys. (France) Lett. **41**, L344 (1980); M. Dubois, M.A. Rubio, and P. Berg, Phys. Rev. Lett. **51**, 1446 (1983); J.Y. Huang and J.J. Kim, Phys. Rev. A **36**, 1495 (1987).

[2] P. Manneville and Y. Pomeau, Phys. Lett. **75A**, 1 (1979).

[3] B. Hu and J. Rudnick, Phys. Rev. Lett. **48**, 1645 (1982).

[4] O.J. Kwon, C.M. Kim, E.K. Lee, and H. Lee, Phys. Rev. E **53**, 1253 (1996); C.M. Kim and W.H. Kye, *ibid.* **63**, 037202 (2001).

[5] H.G. Schuster, *Deterministic Chaos*, 2nd ed. (VCH, Weinheim, 1987).

[6] C.M. Kim, O.J. Kwon, E.K. Lee, and H. Lee, Phys. Rev. Lett. **73**, 525 (1994).

[7] C.M. Kim, G.S. Yim, Y.S. Kim, J.M. Kim, and H.W. Lee, Phys. Rev. E **56**, 2573 (1997).

[8] C.M. Kim, G.S. Yim, J.W. Ryu, and Y.J. Park, Phys. Rev. Lett. **80**, 5317 (1998).

[9] E. Ott, *Chaos in Dynamical Systems* (Cambridge University Press, Cambridge, England, 1993).

[10] J.P. Eckmann, L. Thomas, and P. Wittwer, J. Phys. A **14**, 3153 (1982).

[11] J.E. Hirsch, B.A. Huberman, and D.J. Scalapino, Phys. Rev. A **25**, 519 (1982).

[12] J.E. Hirsch, M. Nauenberg, and D.J. Scalapino, Phys. Lett. **87A**, 391 (1982).

[13] W.H. Kye and C.M. Kim, Phys. Rev. E **62**, 6304 (2000).

[14] D.J. Biswas, V. Dev, and U.K. Chatterjee, Phys. Rev. A **35**, 456 (1987).

[15] C.M. Kim, K.S. Lee, J.M. Kim, S.O. Kwon, C.J. Kim, and J.M. Lee, J. Opt. Soc. Am. B **10**, 1651 (1993).

[16] J.P. Crutchfield, J.D. Farmer, and B.A. Huberman, Phys. Rep. **92**, 45 (1982).

[17] C.W. Gardiner, *Handbook of Stochastic Methods*, 2nd ed. (Springer-Verlag, New York, 1985); H. Risken, *The Fokker-Planck Equation*, 2nd ed. (Springer-Verlag, New York, 1996) (for the correspondence between the stochastic differential equation and FPE, see Secs. 3.6, 4.3, and 5.2 of the first book).

[18] E.R. Hunt, Phys. Rev. Lett. **49**, 1054 (1982); R.W. Rollins and E.R. Hunt, *ibid.* **49**, 1295 (1982); S.D. Brorson, D. Dewey, and P.S. Linsay, Phys. Rev. A **28**, 1201 (1983); C.M. Kim, C.H. Cho, C.S. Lee, J.H. Yim, J. Kim, and Y. Kim, *ibid.* **38**, 1645 (1988).